JOURNAL OF AIRCRAFT
Vol. 32, No. 6, November–December 1995

Real-Time Model of Three-Dimensional Dynamic Reattachment Using Neural Networks

William E. Faller,* Scott J. Schreck,† and Hank E. Helin‡
U.S. Air Force Academy, Colorado Springs, Colorado 80840

The reattachment of unsteady separated flowfields is a critical issue in the determination of both helicopter and wind-turbine blade performance as well as for poststall maneuvers in aircraft. To fully understand this process and to enable control, numerical techniques that provide real-time models of the reattachment process over a broad parameter range must be realized. This article describes real-time models, using neural networks, for the dynamic reattachment of three-dimensional unsteady separated flowfields. The results indicate that the neural network model accurately predicts the dynamic reattachment process to within 5% of the experimental data across the parameter space bounded by nondimensional pitch rates α^+ of 0.01 and 0.20. However, the error was substantially larger for an α^+ of 0.02. Analyses indicate that the parameter space is governed by two different sets of flow physics that transition at roughly an α^+ of 0.03. As such, the results show that neural network models can be used not only to detect changes in the flow physics, but for defining areas within the parameter space where additional experimental characterization would be useful. Further, the results indicate that the flowfield wing interactions are three dimensional, however, the spanwise effects of the three dimensionality are subdued relative to dynamic stall.

Nomenclature

C_d = drag coefficient
C_l = lift coefficient
C_m = one-quarter chord moment coefficient
C_n = normal force coefficient
C_t = tangential force coefficient
c = wing chord length, cm
c_p = pressure coefficient
$d\alpha/dt$ = pitch rate, rad/s
t = time, s
t_{nd} = nondimensional time, $t^* U_\infty/c$
U_∞ = test section velocity, m/s
α^+ = nondimensional pitch rate, $c(d\alpha/dt)/U_\infty$

Introduction

RESEARCH in the area of unsteady flows continues to be strongly motivated by potential enhancements to helicopter, wind-turbine, and aircraft performance. Helicopter and wind-turbine blades experience force and moment histories that are dependent on both dynamic stall as well as on the subsequent reattachment of the flowfield. Additionally, the dynamic reattachment of unsteady separated flowfields has been highlighted as a major concern for rapidly maneuvering aircraft.[1]

The three dimensionality inherent to practical geometries as well as the time dependence of unsteady separated flows renders them highly complex. For dynamic stall, spanwise nonuniformities in vortex structure and kinematics give rise to spanwise variations in surface pressure distribution and normal force coefficient.[2–5] Similar spanwise nonuniformities and time-dependent variations in surface pressure distribution have been shown for the dynamic reattachment of unsteady separated flowfields.[6–9]

This temporal and spatial complexity, in turn, yields a phenomenon that is very difficult to thoroughly characterize. As such, the broad parameter space encompassed by three-dimensional unsteady separated flows has defied comprehensive description. However, neural network models that accurately predict, and describe mathematically, three-dimensional unsteady surface pressure topologies as well as the aerodynamic coefficients have been described.[10–13] Further, the neural network models were shown to be accurate throughout the complete time history of the maneuver. Building upon these techniques, real-time models for dynamic reattachment of three-dimensional unsteady separated flowfields were developed.

Methods

Unsteady Surface Pressure Measurement

Surface pressure measurements were performed in the Frank J. Seiler 0.91 m × 0.91 m low-speed wind tunnel located at the U.S. Air Force Academy. A rectangular planform wing (NACA 0015 cross section), having a span of 30.48 cm and a semiaspect ratio of 2.0 was bounded at the root by a circular splitter plate. Fifteen Endevco 8507-2 miniature pressure transducers were close coupled to the wing surface through 15 pressure ports located along the chord line. The 15 transducers were located between 0% chord, the leading edge, and 90% chord. Using wingtip extensions these 15 pressure transducers were moved to 3 spanwise positions located at 0% span (the wing root), 37.5% span, and 80% span near the wingtip. This is shown schematically in Fig. 1. In all tests, wind-tunnel test section velocity was held constant at 9.14 m/s, corresponding to a chord Reynolds number of 6.9×10^4.

Starting at 60 deg, from a fully stalled condition, the wing/splitter plate configuration was pitched down at a constant rate (about the wing quarter chord) to a final angle of 0 deg. Pitch rates $d\alpha/dt$ of 34, 68, 172, 258, 344, 516, and 688 deg/s were employed. This corresponded to nondimensional pitch rates α^+ of 0.01, 0.02, 0.05, 0.075, 0.10, 0.15, and 0.20. Pitch angle histories for these records are shown in Fig. 2.

Presented as Paper 94-2337 at the AIAA 25th Fluid Dynamics, Plasmadynamics, and Lasers Conference, Colorado Springs, CO, June 20–23, 1994; received Aug. 1, 1994; revision received April 12, 1995; accepted for publication April 12, 1995.

*Research Faculty; currently at Johns Hopkins University, Department of Mechanical Engineering, David Taylor Model Basin, Code 54, Carderock Division, Naval Surface Warfare Center, Bethesda, MD 20084-5000. Member AIAA.

†Unsteady Aerodynamics Task Manager, Frank J. Seiler Research Laboratory. Member AIAA.

‡Faculty, Department of Aeronautics. Member AIAA.

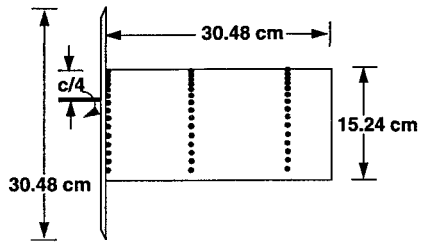

Fig. 1 Pressure transducer locations both along the chord and spanwise on the wing.

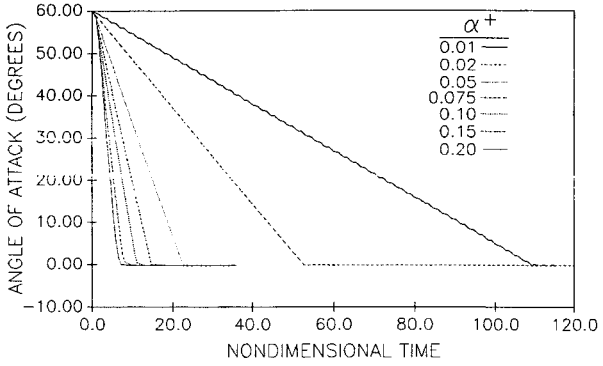

Fig. 2 Wing motion histories for the seven pitch-down cases.

A total of 21 combinations of nondimensional pitch rate and spanwise pressure port location were recorded. Signals originating from the pressure transducers were sampled at 500 Hz and digitized yielding surface pressure records comprised of 200 samples per transducer for nondimensional pitch rates of 0.05–0.20. The surface pressure records for nondimensional pitch rates of 0.01 and 0.02 were comprised of 1000 data points. For each record, 20 consecutive wing pitch motions were sampled and ensemble averaged to arrive at the final surface pressure data set. Note, because of the relatively small magnitude of the pressure readings, a factor of 5–10 smaller than for dynamic stall, the signal reflects mechanical vibrations in some instances, despite ensemble averaging. Following acquisition, the surface pressure values were converted to pressure coefficients c_p. A detailed explanation of the methods for experiments based on both pitch-up and pitch-down motions have previously been described.[3,4,9]

Figure 3 shows a representative set of ensemble-averaged experimental data for one pitch rate ($\alpha^+ = 0.05$) at one span location (the wing root). The abscissa is nondimensional time and the ordinate is surface pressure. The relative magnitudes of the pressure traces are accurate, but the traces have been offset to ease viewing. Each pressure signature corresponds to the data record obtained from a single pressure port location, leading edge at the bottom of the figure, and 90% chord at the top of the figure. Flowfield reattachment at each pressure port location has been circled. As shown below the figure, each of the pressure signatures was comprised of 200 data points.

Neural Network Model

For all nondimensional pitch rates, prominent temporal and spatial variations in the surface pressure topology were apparent. To incorporate these characteristics, a simplified model comprised of three span locations (0, 37.5, and 80% span) was developed. The neural network model (architecture) is shown schematically in Fig. 4. A standard sigmoidal activation function, $1/(1 + e^{-x})$, was used and the inputs to the network were the time-varying pitch angle α, angular velocity $d\alpha/dt$, and the surface pressure initial conditions at time t_0. The model was trained on 5 of the 7 data records corresponding

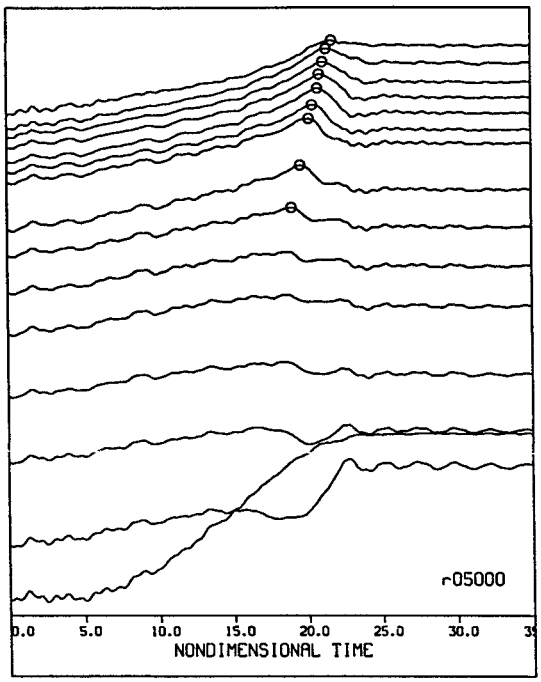

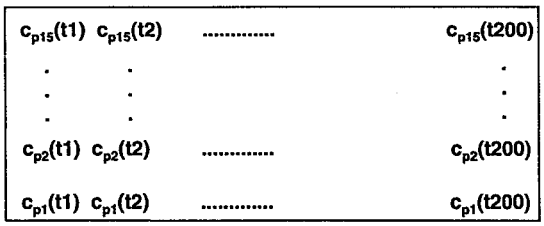

Fig. 3 Raw data for a single pitch history. Each of the 15 pressure traces was comprised of 200 data points.

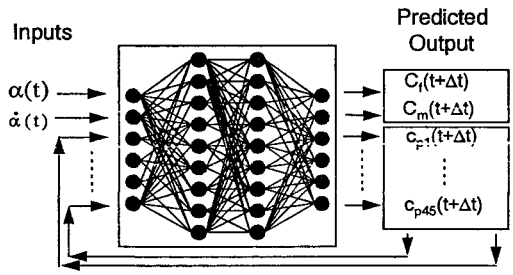

Fig. 4 The neural network model. Inputs were α, $d\alpha/dt$, and $t + \Delta t$ fed back as inputs throughout the pitch history.

to nondimensional pitch rates of 0.01, 0.02, 0.05, 0.10, and 0.20, using a time-series algorithm based on backpropagation. The input vector was comprised of 47 values. Both hidden layers were comprised of 32 units and the output layer was comprised of 60 units. The targeted outputs were the surface pressure values at time $(t + \Delta t)$ for each of the 45 surface pressure records as well as the 15 aerodynamic coefficients, (C_l, C_d, C_n, C_t, and C_m), for each of the three span locations modeled. Subsequently, to maintain the time dependence of the flowfield, the time $(t + \Delta t)$ network predictions for each of the 45 surface pressures were fed back as inputs to the network throughout the pitch history. This type of neural network model has previously been described in detail for predictions of dynamic stall.[10–13] Reasonably complete descriptions of both the mathematics and techniques for neural networks used in both modeling and control are also available.[14–16]

Results

To evaluate the performance of the model, the predicted surface pressures were compared directly to the measured ensemble-averaged data. The only external inputs provided to the model were the instantaneous pitch angle α and the angular velocity $d\alpha/dt$. The internal inputs to the model were the time $(t + \Delta t)$ predicted surface pressures that were fed back as inputs to maintain the time-dependence of the flowfield. With this posttraining it was possible to accurately determine not only how well the model predicted the training data, but how well the model could predict dynamic reattachment for a broad range of pitch-down motions not used during training.

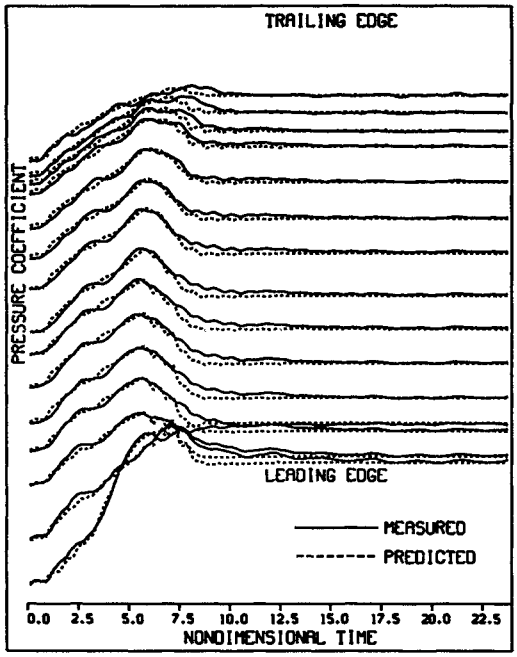

Fig. 5 Surface pressures for nondimensional pitch rate 0.20 at 0% span.

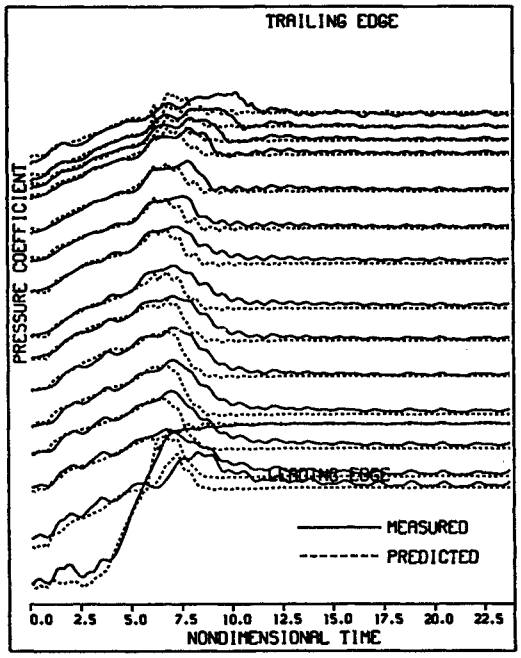

Fig. 6 Surface pressures for nondimensional pitch rate 0.20 at 37.5% span.

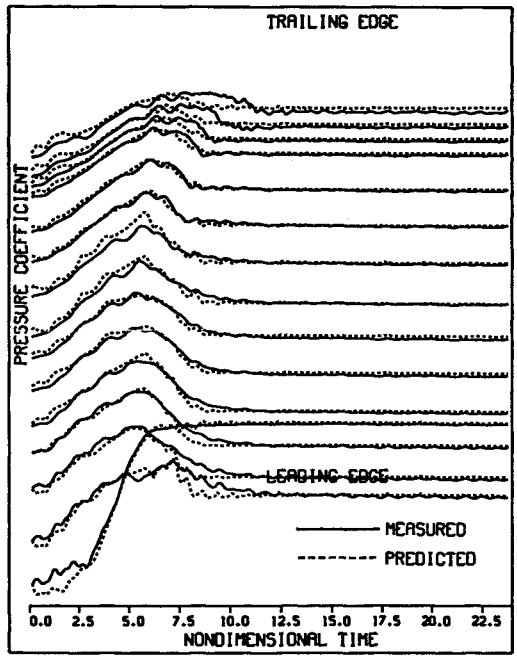

Fig. 7 Surface pressures for nondimensional pitch rate 0.20 at 80% span.

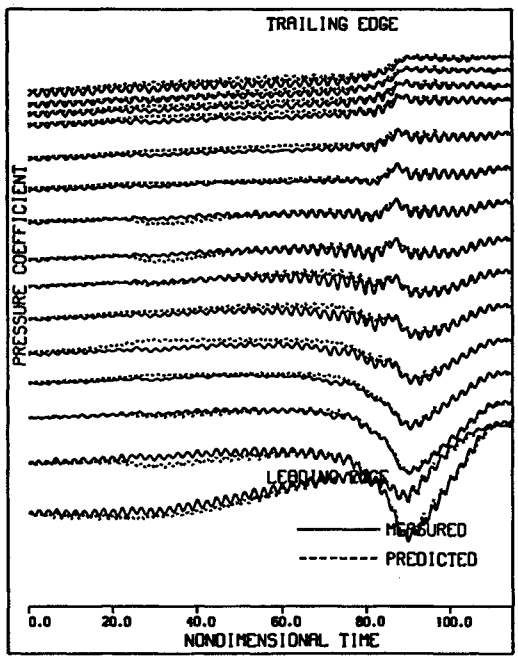

Fig. 8 Surface pressures for nondimensional pitch rate 0.01 and 0% span.

Graphical analyses of the model-predicted surface pressures are shown in Figs. 5–10. In all figures, time-varying surface pressure at port 1, the leading edge, is at the bottom of the figure. Time-varying surface pressure at port 15, 90% chord, is at the top. The ordinate is the surface pressure and the abscissa is nondimensional time. The measured surface pressure data are shown as a solid line and the surface pressures predicted via the neural network model are shown as a dashed line. The relative magnitudes of the pressure coefficients are accurate, but the plots have been offset to ease viewing.

In all figures, the wing starts at 60-deg angle of attack (nondimensional time 0.0) and is pitched down to 0-deg angle of attack. In response to decreasing wing pitch angle, surface pressures initially increase along the entire wing chord. The

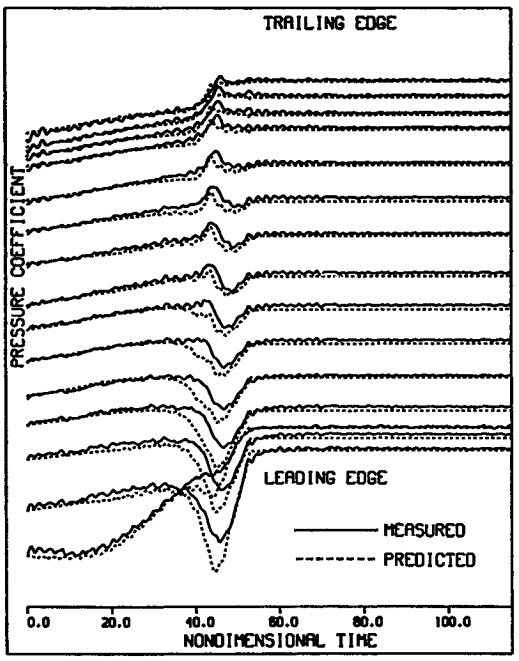

Fig. 9 Surface pressures for nondimensional pitch rate 0.02 and 0% span.

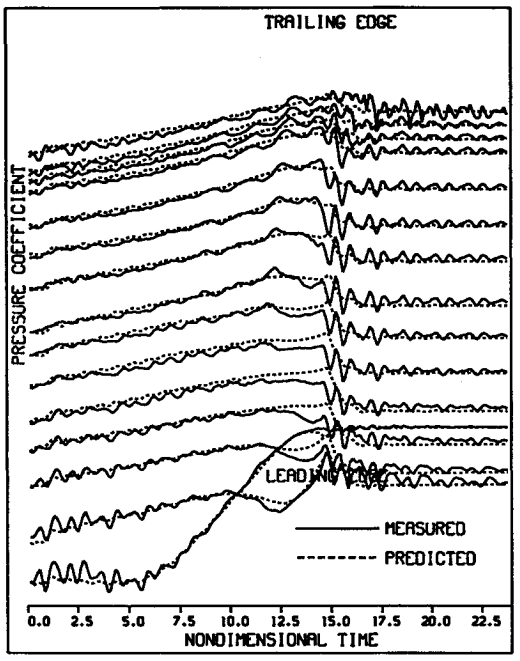

Fig. 10 Surface pressures for nondimensional pitch rate 0.075 and 37.5% span.

increase in surface pressure is then followed by a surface pressure decrease. This decrease in surface pressure, which proceeds from the leading-edge region to the trailing edge of the wing, indicates incipient flowfield reattachment. In Fig. 3 this pressure reversal, indicative of reattachment, was circled at each pressure port location.[6,7]

The analyses for a nondimensional pitch rate of 0.2 at each of the three span locations (0, 37.5, and 80%) are shown in Figs. 5–7. In Fig. 5, at the wing root, prior to the occurrence of the pressure reversal, the model accurately predicted the surface pressure increases at all port locations. At the pressure reversal, the model accurately predicted the time and magnitude of dynamic reattachment. Similarly, in Figs. 6 and 7, at 37.5 and 80% span, the model accurately predicted the initial surface pressure increases. However, as shown in Fig. 6, the time of occurrence and the magnitude of the pressure reversal were not well predicted at the 37.5% span location. At 80% span, both the time of occurrence and magnitude of the pressure reversal were accurately predicted.

The analysis for a nondimensional pitch rate of 0.01, at the wing root, is shown in Fig. 8. Initial pressure values were overpredicted near the leading edge and underpredicted near the trailing edge. However, the model accurately predicted the time of occurrence and magnitude of the pressure reversal at all port locations. The magnitude and time of occurrence of the pressure peak occurring at nondimensional time 90.0, near the leading edge, was also accurately predicted. Similar results were obtained for the remaining two records in the simplified three-dimensional flowfield (37.5 and 80% span). However, as shown previously for a nondimensional pitch rate of 0.2, prediction accuracy was decreased for the surface pressure distribution at 37.5% span as compared to both 0 and 80% spans.

The analysis for a nondimensional pitch rate of 0.02, at the wing root, is shown in Fig. 9. The initial surface pressure rise was overpredicted. The predicted time of the pressure reversal occurs earlier than in the experimental data. In addition, the magnitude of the pressure peak (nondimensional time 45.0) was substantially overpredicted. Similar results were obtained for the remaining two records in the simplified three-dimensional flowfield at 37.5 and 80% spans.

Figure 10 shows a similar plot for a nondimensional pitch rate of 0.075 at the 37.5% span location. This record was not used during training. Near the leading edge the model accurately predicted the initial pressure rise, while near the trailing edge the network underpredicted the surface pressure values. The time of flowfield reattachment was accurately predicted by the model, however, the magnitude of the pressure reversal was underpredicted. As shown previously, the records at 0 and 80% spans were predicted more accurately by the model.

To maintain uniformity with the surface pressure data, the accuracy of the neural-network-predicted aerodynamic coefficients was verified graphically. The graphical analyses for predicting both training data as well as for a data set not used during training are shown in Figs. 11 and 12, respectively. In

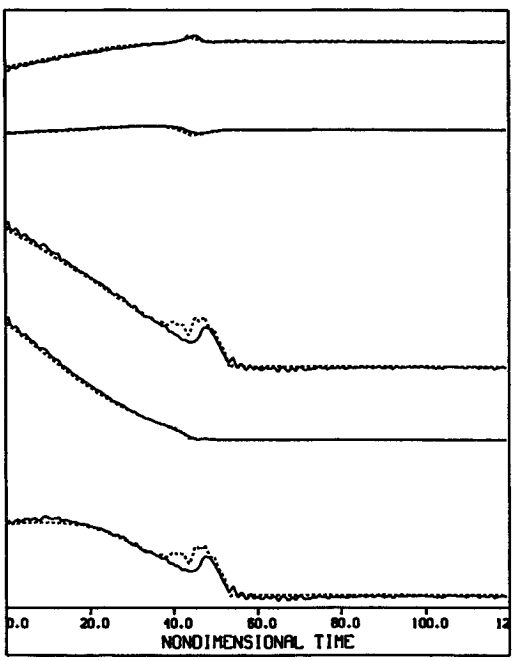

Fig. 11 Aerodynamic coefficients for nondimensional pitch rate 0.02 at 0% span. Bottom to top, C_l, C_d, C_n, C_t, and C_m.

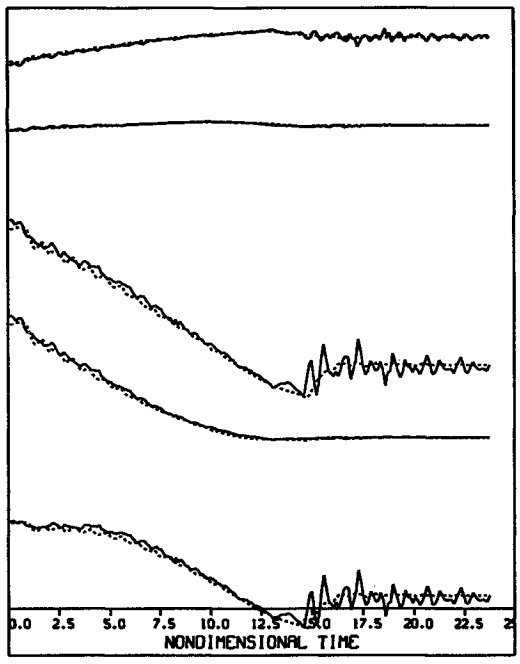

Fig. 12 Aerodynamic coefficients for nondimensional pitch rate 0.075 at 37.5% span. Bottom to top, C_l, C_d, C_n, C_t, and C_m.

both figures, the abscissa is nondimensional time and the ordinate corresponds to the aerodynamic coefficients. The measured data is shown as a solid line and the aerodynamic coefficients predicted by the neural network model are shown as a dashed line. Again, the relative magnitudes of the aerodynamic coefficients are accurate, but the plots have been offset to ease viewing. Starting at the bottom of the figure and proceeding to the top, the aerodynamic coefficients shown are C_l, C_d, C_n, C_t, and C_m.

The analysis for a nondimensional pitch rate of 0.02, at 0% span, is shown in Fig. 11. The neural network accurately predicted both the drag and tangential coefficients as well as the pitching moment coefficient throughout the pitch history. However, consistent with the overprediction of the surface pressure peak, the model overpredicted the magnitudes of both the normal and lift coefficients. Figure 12 shows the analysis for a nondimensional pitch rate of 0.075 at the 37.5% span location. This record was not used during training. For these conditions, the time of occurrence of peak magnitudes was accurately predicted in all cases. However, the magnitude of the peak normal and lift forces was slightly underpredicted.

Overall, as measured by a time-averaged deviation, the model accurately predicted the unsteady surface pressure distributions as well as the aerodynamic coefficients to within 5% of the experimental data. Consistent results were obtained both for the training data as well as for generalization to other constant pitch rates. These results strongly suggest that the neural network model can accurately predict dynamic reattachment. However, as shown, the error was substantially larger for a nondimensional pitch rate of 0.02. These results suggest that the flow physics change dramatically in this region of the parameter space. A more detailed experimental characterization, of this region, appears warranted in order to fully describe the flow physics.

Discussion

Unsteady surface pressure readings were obtained from a wing started at 60-deg angle of attack and pitched down to 0-deg angle of attack. All records showed extensive alterations in the three-dimensional dynamic reattachment as a function of both nondimensional pitch rate and span location. Five of seven records were used to train the neural network. Following training, the model was required to predict the flowfield dynamic reattachment based solely on the wing motion history.

The analyses for predicting a nondimensional pitch rate of 0.20 at 0, 37.5, and 80% span were shown in Figs. 5, 6, and 7, respectively. The analysis for predicting a nondimensional pitch rate of 0.01 at the 0% span location was shown in Fig. 8. All of these data sets were used in training the neural network. In all of the figures, the overlaid plots indicated that the neural network accurately modeled dynamic reattachment. Additionally, all results indicated that the neural network accurately predicted the pressure reversal, at each port location, which was characteristic of the flow reattachment. Interestingly, the reattachment process at the 37.5% span location was the most difficult case for the neural network to model. Based on previous results for dynamic stall, it was anticipated that the 37.5% span location would have provided the most accurate predictions.

The result for a nondimensional pitch rate of 0.02 was shown in Fig. 9. In this case, it was clear that the model could not predict the surface pressure peak that occurred at a nondimensional time 45.0. This pressure peak was also evident for a nondimensional pitch rate of 0.01, at a nondimensional time of 90.0, but not for α^+ of 0.05 or higher. As shown in Fig. 13, the magnitude of the pressure peak falls off nonlinearly from a maximum, at an α^+ of 0.01, to a value of zero at an α^+ of 0.05. Since the model has only two examples where this pressure peak occurs, and the fall-off in magnitude is nonlinear, the end result is that the model overpredicted the magnitude of the pressure peak for an α^+ of 0.02. This is a case where additional data in the α^+ range of 0.02–0.04 would be useful in order to better characterize the change in flow physics that occurs in this region of the parameter space. Note, a priori, there was no way to know if this additional experimental characterization would be justified or needed.

The analysis for predicting a nondimensional pitch rate of 0.075 at the 37.5% span location is shown in Fig. 10. This data set was not used in training the neural network. The results indicated that the neural network accurately predicted the unsteady flowfield reattachment. Both magnitudes and pressure reversal times were generally well predicted. Thus, for data records not used during training, the neural network model was able to predict the dynamic reattachment process.

Similar results were obtained for the prediction of the aerodynamic forces and moments. The analysis for predicting the aerodynamic coefficients associated with a nondimensional pitch rate of 0.02 was shown in Fig. 11. Consistent with the results described for the surface pressures, the peak magnitudes of the normal and lift forces were overpredicted. Figure 12 showed the analysis for an α^+ of 0.075 at the 37.5% span location. This data set was not used in training the neural network. Again, the results indicated that the neural network accurately predicted both the magnitude and time-dependent history of the aerodynamic coefficients. Consistent with the results for the surface pressure distributions shown earlier, the neural network was shown to accurately model the aerodynamic coefficients across a wide range of nondimensional pitch rates.

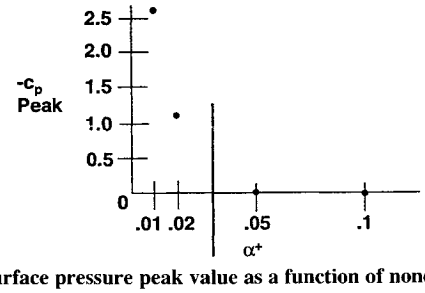

Fig. 13 Surface pressure peak value as a function of nondimensional pitch rate.

Overall, as measured by a time-averaged error, the results indicated that the network accurately modeled three-dimensional dynamic reattachment to within 5% of the experimental data. These results support the previous indication, from dynamic stall models, that highly accurate real-time models of unsteady separated flowfields can be developed using neural networks. Further, these results strongly suggest that such models can be used to detect changes in the flow physics as well as for defining areas within the parameter space where additional experimental characterization would be useful.

Conclusions

Unsteady surface pressure readings, for seven nondimensional pitch rates, were obtained from a wing started at 60-deg angle of attack and pitched down to 0-deg angle of attack. All records showed extensive alterations in the three-dimensional unsteady reattachment as a function of both nondimensional pitch rate and span location. Using this data, neural network models for three-dimensional dynamic reattachment were developed. Following training, the inputs to the network were the α, $d\alpha/dt$, and t_0. Subsequently, to maintain the time dependence of the flowfield, the time $(t + \Delta t)$ network predictions for each of the 45 surface pressures were fed back as inputs to the network throughout the pitch history. The results clearly indicated that except for the initial conditions, the model did not require any measured data in order to predict dynamic reattachment. Overall, as measured by a time-averaged error, the results indicated that the network accurately modeled three-dimensional dynamic reattachment to within 5% of the experimental data.

The results for a nondimensional pitch rate of 0.02, shown in Fig. 9, provided a clear example of a case where additional data in the range of α^+ 0.02–0.04 would be useful in order to better characterize the transition in flow physics. Note, a priori, that there was no way to know if this additional experimental characterization would be justified or needed. As such, these results indicate that such models can be used not only to detect changes in the flow physics, but for defining areas within the parameter space where additional experimental characterization would be useful.

As shown herein, the real-time prediction of dynamic reattachment for three-dimensional unsteady separated flowfields and aerodynamic coefficients can readily be attained using neural networks. Further, these results were shown to span an extremely broad parameter range. Similar results have previously been shown for the real-time prediction of dynamic stall.[12,13] Accurate, real-time predictions of three-dimensional unsteady separated flowfields should facilitate the development of control systems for improving helicopter and wind-turbine performance, as well as for enhancing aircraft agility.

References

[1]Ericsson, L. E., "Pitch-Down Dynamic Stall Characteristics," AIAA Paper 94-0535, Jan. 1994.

[2]Robinson, M., Walker, J., and Wissler, J., "Unsteady Surface Pressure Measurements on a Pitching Rectangular Wing," *Proceedings of Workshop II on Unsteady Separated Flow*, U.S. Air Force Academy, CO, 1988, pp. 225–237.

[3]Schreck, S., Addington, G., and Luttges, M., "Flow Field Structure and Development Near the Root of a Straight Wing Pitching at Constant Rate," AIAA Paper 91-1793, June 1991.

[4]Schreck, S., and Helin, H., "Unsteady Vortex Dynamics and Surface Pressure Topologies on a Pitching Wing," AIAA Paper 93-0435, Jan. 1993.

[5]Lorber, P., Covino, A., and Carta, F., "Dynamic Stall Experiments on a Swept Three-Dimensional Wing in Compressible Flow," AIAA Paper 91-1795, June 1991.

[6]Niven, A. J., Galbraith, R. A. McD., and Herring, D. G. F., "Analysis of Reattachment During Ramp-Down Tests," *Vertica*, Vol. 13, No. 2, 1989, pp. 187–196.

[7]Niven, A. J., and Galbraith, R. A. McD., "Experiments on the Establishment of Fully Attached Aerofoil Flow from the Fully Stalled Condition During Ramp-Down Motions," International Council of the Aeronautical Sciences, ICAS Paper 90-3.4.3, March 1990.

[8]Ahmed, S., and Chandrasekhara, M. S., "Reattachment Studies of an Oscillating Airfoil Dynamic Stall Flow Field," AIAA Paper 91-3225, Sept. 1991.

[9]Schreck, S. J., Faller, W. E., and Helin, H. E., "Dynamic Reattachment on a Downward Pitching Finite Wing," AIAA Paper 94-3426, June 1994.

[10]Faller, W. E., Schreck, S. J., and Luttges, M. W., "Quasi-Linear Neural Networks: Application to the Prediction and Control of Unsteady Aerodynamics," Society of Photo-Optical Instrumentation Engineers, SPIE Paper 1965-40, May 1993.

[11]Schreck, S. J., Faller, W. E., and Luttges, M. W., "Neural Network Prediction of Three-Dimensional Unsteady Separated Flow Fields," AIAA Paper 93-3426, Aug. 1993.

[12]Faller, W. E., Schreck, S. J., and Luttges, M. W., "Real-Time Prediction of Unsteady Aerodynamics: Application for Aircraft Control and Maneuverability Enhancement," *IEEE Transactions on Neural Networks* (to be published).

[13]Faller, W. E., Schreck, S. J., and Luttges, M. W., "Real-Time Prediction and Control of Three-Dimensional Unsteady Separated Flow Fields Using Neural Networks," AIAA Paper 94-0532, Jan. 1994.

[14]Fausett, L., *Fundamentals of Neural Networks: Architectures, Algorithms and Applications*, ISBN 0-13-334186-0, Prentice–Hall, Englewood Cliffs, NJ, 1994.

[15]Haykin, S., *Neural Networks: A Comprehensive Foundation*, ISBN 0-02-352761-7, Macmillan, New York, 1994.

[16]Miller, W. T., III, Sutton, R. S., and Werbos, P. J. (eds.), *Neural Networks for Control*, ISBN 0-262-13261-3, Massachusetts Inst. of Technology Press, Cambridge, MA, 1990.